A Guide-Wired Helical Microrobot for Mechanical Thrombectomy: A Feasibility Study

Kim Tien Nguyen, Gwangjun Go, Eunpyo Choi, Byungjeon Kang, Jong-Oh Park*, *Member, IEEE*, and Chang-Sei Kim*, *Member, IEEE*

***Abstract*— In this paper, we present a novel guide-wired helical microrobot for mechanical thrombectomy in cardio-vascular system, especially for calcified thrombus therapeutics. We designed and fabricated a prototype of the helical shape microrobot equipped with a freely rotatable spherical joint connected to a catheter guidewire, that enables drilling capability to remove calcified objects in vascular. The guidewire helps supporting and maneuvering the microrobot against blood flow during thrombus removal procedure. In addition to the microrobot, an enhanced electromagnetic navigation system (ENS) is implemented to utilize high frequency operation based on resonant effect, which enables powerful drilling force of the microrobot. The in-vitro experimental results illustrate that the suggested method could successfully enhance the locomotion and the drilling force of the helical microrobot that would be sufficient for future mechanical thrombectomy application in cardiovascular therapeutics.**

I. Introduction

The mechanical thrombectomy has been proposed to increase revascularization [1] as a surrogate for intravascular therapeutics of tissue plasminogen activator (tPA) which is restrictive time window after stroke onset and less effective in large vessel treatment [2]. As an outcome of the mechanical thrombectomy utilizing advanced catheterization technology such as Merci retriever with a corkscrew distal wire [3] or balloon catheterization [4], Solitaire stent retriever [5], and direct aspiration [6], the recanalization rate could be achieved higher and faster than before. However, intravascular procedures utilizing those devices require very skillful operators for the improvement of patient outcomes. In addition, the risk related to the operator's exposure to radiation is presented as a critical disadvantage, since they have to directly operate under X-ray monitoring devices.

In order to overcome those problems and accomplish remote operations, the magnetically steering guidewire controlled by the electromagnetic navigation system (ENS) have appeared and are increasingly considered as a promising approach by its advantages of wireless actuation, multi degree of freedom controllability, strong actuation force, modifiable size and shape, and low cost [7]. Many researches have been pursued in an effort to control the guidewire equipped with a small permanent magnet on the guidewire tip by using ENS [8]–[11]. The forward and backward motion of the magnetic guidewire was applied to break thrombus by the motorized feeding device. However, this method couldn't successfully pass through the thrombus due to the low stiffness of the guidewire. Hence the magnetic helical microrobot was suggested as a suitable alternative, since it showed the capability of drilling and moving by converting the applied electromagnetic torque into propulsion force with externally applied rotating magnetic field. That has more advantages for removal of thrombus in blood vessel [12]–[17]. But, in the in-vivo experiments, generating enough propulsion force and drilling torque for helical microrobot to move into the target region and to stand stable during drilling procedure against fast blood flow were very challenging. In addition, the high-frequency alternating electromagnetic fields was required for ENS to generate the stable locomotion and strong drilling force of helical microrobot. However, in the conventional ENS, the high-frequency of the input voltage strongly affected the coil impedance and phase delay which deteriorated the magnetic force and controllability, and for some cases, the required input voltage to the system was exceed the available maximum power and result in excessive power consumption. Nam *et al*. proposed a series of capacitors connected to the coils, which can compensate phase delay for a frequency of up to 75 Hz, but it has a limitation of manual frequency switching for a specific range [18]. Eventually, to accomplish the successful implementation of the intravascular microrobot for mechanical thrombectomy, both strong electromagnetic field and stable helical microrobot motions against blood flow need to be conquered.

This paper aims to address a feasible methodology of the mechanical thrombectomy procedure. The contributions are a novel helical microrobot mechanism equipped with a spherical joint and a guide-wire that can improve steering force, and an enhanced ENS. A helical microrobot fabricated with a freely rotatable spherical joint connected to a guidewire could perform drilling, steering, and propulsion capabilities against strong blood flow in vessels. In addition, the enhanced ENS consists of a resonant control circuit and an automatic pseudo-continuous capacitance switching method is developed. That can maintain high-current at a wide range of operation frequency. This method can smoothly control microrobot's drilling motion. In-vitro experimental results also will be provided to show the feasibility of the suggested mechanical thrombectomy system for the clinical application in practice.

II. System Overview

For the perspective of the practical fully controllable helical microrobot with guidewire implementation in the

*Research supported in part by the Bio & Medical Technology Development Program of the National Research Foundation (NRF) funded by the Korean government (MSIT) (No. 2015M3D5A1065682)

K. T. Nguyen, E. Choi, J.-O. Park*, and C. S. Kim* are with the School of Mechanical Engineering, Chonnam National University, Gwangju 61186, South Korea (e-mail: nguyenkimtien90@gmail.com; eunpyochoi@chonnam.ac.kr; jop@jnu.ac.kr; ckim@jnu.ac.kr).

B.J. Kang, G. Go is with the Medical Microrobot Center, Robot Research Initiative, Chonnam National University, Gwangju 61011, South Korea (e-mail: bjkang8204@jnu.ac.kr, gwangjun124@gmail.com).

blood vessel, the overall system utilized in this study is composed of a helical microrobot, an ENS, and an imaging system as depicted in Fig. 1. The microrobot is externally controlled by ENS. The microrobot is remotely controlled by a clinician outside of the operating room where the clinician can avoid X-ray exposure. The key factors of each part are explained in this section, as followings.

A. Intravascular helical microrobot for drilling

For the effective locomotion and drilling motion of the microrobot in blood vessel, the microrobot is designed to have a helical or spiral shape. The geometric size of the robot needs to be minimized that can be inserted into the blood vessel by considering the locomotion. A small permanent magnet is placed inside the robot body that can interact with the external ENS for the purpose of generating high force and torque to realize sufficient locomotion and drilling motion. The magnetization direction of the microrobot is also an important factor to be considered that is related with the motion control.

B. ENS system for external actuation

The ENS plays an important role to generate a sufficient magnetic field to produce torque to align the microrobot and force to drive the microrobot in 3-dimensional (3D) space by fully utilizing uniform magnet field and gradient magnet field. In our previous works, we had successfully demonstrated several different configuration and size of ENS based on air-core type electromagnets with capability of microrobot's 3D locomotion depending on microrobot applications [12] [13] [15] [16].

C. Imaging system for microrobot tracking

Last but not least, tracking and recognition of the robot orientation and position in human body is an important issue for clinical application. That is related to the microrobot's targeting accuracy and intravascular intervention safety during the mechanical thrombectomy procedure and the further remote control application. Since the X-ray fluoroscopy is currently available in the operating room, we utilize the X-ray imaging system in this study. As a promising alternative, MRI system can be used to manipulate and to recognize the object, simultaneously. But, the relatively small driving magnetic force in the vessel has been presented that is caused by the scanning sequencing for image monitoring conflicts with magnetic field control for microrobot motion. Hence, an imaging system is equipped with the capability of localization and detection of the microrobot by utilizing bi-plane X-ray fluoroscopy with three dimensional object reconstructions as shown in Fig. 2 (b) and (c).

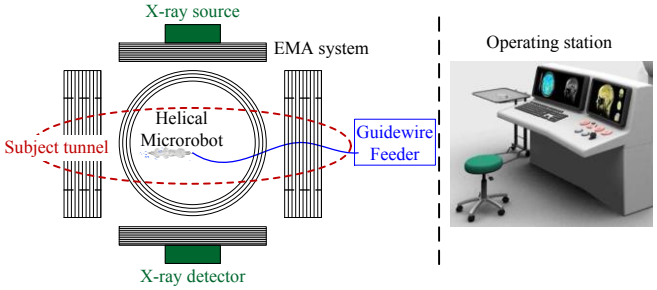

Figure 1. Schematics of the suggested guide-wired helical microrobot system.

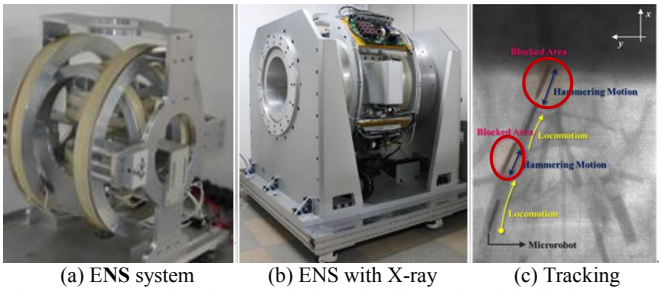

(a) ENS system (b) ENS with X-ray (c) Tracking

Figure 2. Conventional ENS platform in this study with bi-plane X-ray fluoroscopy and tracking in blood vessel [18].

III. Enhanced Helical Microrobot System

In this section, the developed mechanical thrombectomy system with novel mechanism of the guide-wired helical microrobot and the driving power and frequency range enhanced ENS are explained.

A. Guide-wired helical microrobot

Fig.3. (a) shows a structure of the helical shape microrobot and Fig.3. (b) depicts a fabricated prototype made by a 3D printer (VeroClear-RGD810 from Stratasys). The helical microrobot is based on the previous helical microrobot [12]. The developed device is newly equipped with a rotatable spherical joint at the end of the helical microrobot. And the spherical joint is connected to a guidewire. The guidewire connection performs to help supporting the microrobot against blood flow in the vessel. Moreover, the spherical joint can maintain the drilling motion without twisting the supporting guidewire.

The geometric parameters of the fabricated microrobot are summarized in Table I. The body size is minimized to be inserted into the commercially available catheter for artery therapeutics.

TABLE I. Geometric Parameters of Helical-Head Guidewire

Design Parameter	Description	Value
R	Body radius [mm]	1
λ	Helix pitch [mm]	5.5
2r	Spiral thickness [mm]	0.12
	Spiral height [mm]	1.2
	Head length [mm]	12
	Permanent magnet [mm]	1×5

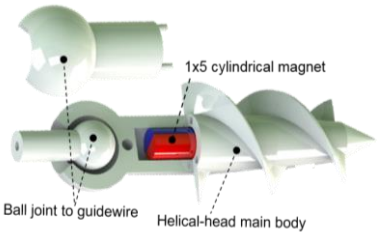

(a)

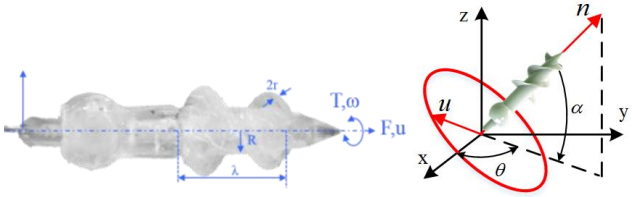

(b) (c)

Figure 3 (a) Structure design, (b) 3D printed helical robot, and (c) locomotion coordinate of the helical robot with the desired rotating electromagnetic field.

A permanent magnet is placed inside the robot body that interacts with the electromagnetic field generated by ENS for motion control. The magnetization orientation of the tip is orthogonal to the body axis. The ball joint is designed to implement the spherical motion connected to the microrobot body with 0.011″ super-elastic commercial guidewire. The guidewire length as well as pushing and retracting motion is controlled by the guidewire feeder.

B. Power and frequency-range improved ENS

Three orthogonal pairs of air-core type electromagnetic coils are used for the ENS that consists of an x-directional circular Helmholtz coil, CHCx, and y- and z-directional two square Helmholtz coils, SHCy and SHCz, respectively. Two pairs of square Helmholtz coil were designed inside the circular Helmholtz coil to maximize the region of interest (ROI). The frame of this proposed system was made of nonconductive materials (Bakelite) to avoid eddy current effects and heat emission. Table II shows the detailed specifications of the developed ENS.

Since the electromagnetic coils are made by copper coil winding, the magnetic flux density reduction and phase delay are unavoidable due to inductance effect. In the conventional ENS, the magnetic flux density showed the dramatically decrease approximately 90% and the phase lag was increased up to 90° with respect to the operating frequency variation of 30Hz to 300Hz. Therefore, to improve the actuation force and widen the operating frequency range of the ENS, it needs to reduce the inductance effect. To eliminate the inductance effect, we design an inductance reduction circuit and a pseudo-continuous switching algorithm by utilizing a variable capacitors circuit, comprised with various capacitors, relays, and switching circuit, in each coil. Assuming that each coil is a simple RL circuit, the variable capacitors circuit to each coil in series forms an RLC equivalent circuit as shown in Fig. 4. Then, the output current of the RLC circuit is computed as followings.

$$I(s) = \frac{sC_v V_i(s)}{LC_v s^2 + RC_v s + 1} \tag{1}$$

And the phase of the RLC circuit is obtained as:

$$\phi = \tan^{-1}\left(\frac{2\pi fL}{R} - \frac{1}{2\pi fRC_v}\right) \tag{2}$$

where C_v is the designed variable capacitor that can match the resonant frequency of the coil system. For the given desired frequency, the capacitor can automatically be switched to match the coil impedance and that can cancel the inductor reactance at the desired frequency. The circuit will resonate at the desired frequency as follows:

$$f_r = \frac{1}{2\pi\sqrt{LC_v}} \tag{3}$$

TABLE II. SPECIFICATION OF THE PROPOSED ENS

Specification	CHCx	SHCy	SHCz
Radius/ length of coil (mm)	162	168	120
Number of turns	472	380	300
Resistance (Ohm)	6.74	9.27	5.42
Inductance (mH)	258	92	37
Magnetic field intensity (A/m)	1982.4	2679.1	2913.3

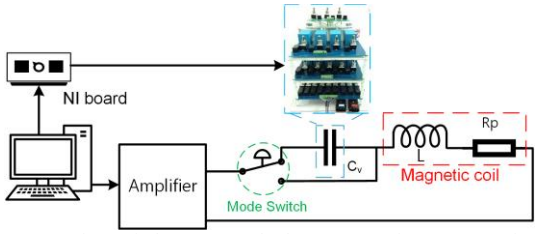

Figure 4. Design of the proposed electromagnetic actuator circuit with resonance control system.

Let $V_L = 2\pi fLI_0$ and $V_C = I_0/(2\pi fC_v)$. By setting the capacitance, $C_v = 1/(2\pi f)^2 L$, the voltages across the coil equals the capacitors voltage, as $V_L = V_C$, and the net voltage across the coil and the resonance control circuit becomes 0 V via the Kirchhoff's voltage law. Since the remaining parasitic resistance was relatively small, the applied voltage to maintain the parasitic resistance can drive the maximum current with a zero phase delay through the ENS at the given input frequency.

IV. RESULTS AND DISCUSSIONS

Fig. 5 demonstrates the widen operating frequency range of the proposed system, in which the controllable lowest to highest resonant frequencies of CHCx, SHCy, and SHCz were 16.58 Hz to 100 Hz, 26.27 Hz to 131.2 Hz, and 41.42 Hz to 370 Hz, respectively. Meanwhile, the proposed ENS can maintain 100% output power at high-frequency range in comparison with the strong reduction of magnetic field at the conventional ENS (as shown in Fig. 5 (a)). The CHCx coil has the lowest maximum operating frequency of 100 Hz, because of its largest inductance value. That necessitated a high voltage to the coil system to maintain a high coil current.

We performed step-out frequency experiment to verify the suggested resonant control circuit. The step-out frequency is directly related to the locomotion speed and drilling efficiency of the microrobot. We continuously increased the rotating magnet field frequency until the microrobot speed dropped down, of which input frequency can be regarded as the limit frequency of the microrobot motion. As a result, the step-out frequency of robot without resonance control system was around 50Hz, but the step-out frequency of the proposed ENS resulted in 200Hz that is much higher than the previous system. We could accomplish 400% improved step-out frequency and the locomotion speed could be improved approximately 388%.

To verify the feasibility of the suggested guide-wired helical microrobot system for mechanical thrombectomy, two in-vitro experiments were conducted; direction control into different branches as shown in Fig. 6 (a), and driving and

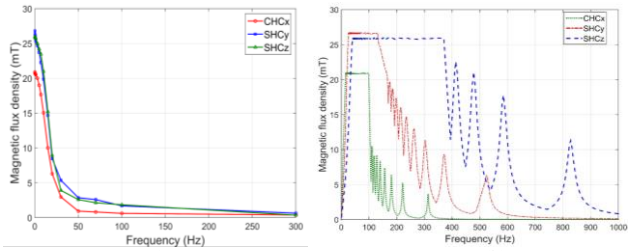

Figure 5. Maximum magnetic flux density and available operating frequency range of (a) conventional ENS, and (b) the proposed ENS system with the series resonance control system.

drilling motion in the water flowing tube as shown in Fig. 6 (b). In Fig. 6 (a), the steering control of the helical microrobot and the obstacle removal motion experiments were carried out for the in-vitro phantom with five branches. First, the guide-wired microrobot was controlled to move into different directions of the phantom branches of 15°, 0°, and -15°. Second, after successful guidewire insertion into the desired branch, the drilling motion and propulsion were performed simultaneously for the effective removal of obstacle. For the mechanical thrombectomy application, a 3D printed phantom was made to mimic the blood vessel environment. We molded an agar-block region (0.5% agarose which was 7 times harder than previous work [12]) at the end of the desired part to mimic the obstacle object in human blood vessel. The developed system could effectively drill through the obstacle within 20s which could demonstrate a significant increase of drilling force. The effect of the guidewire method against flow was evaluated in the water flow tube as shown in Fig. 6 (b). The guide-wired helical robot could maintain its position during drilling motion and move forward and backward freely without influenced by the water flow. Even, it could move forward and backward with simultaneous drilling motion.

V. Conclusions

This study presented the feasiblity of the novel mechanical thrombectomy device by utilizing the guide-wired helical microrobot and the enhanced ENS system. A prototype of the helical microrobot having a spherical joint connected to the guidewire was built up and verified its steering locomotion as well as drilling motions by in-vitro experiment. In addition, the resonance control system to generate the high- frequency and powered electromagnetic field to improve the drilling force was shown for the suggested helical microrobot system. The proposed ENS consisted of the fabricated guide-wired helical microrobot and the enhanced ENS, was experimentally proved its capability of generating a wide range of operation frequency with maximum magnetic field and nearly zero phase delay. Moreover, the motional controllability and drilling forces could be achieved to remove thrombus in the vascular system.

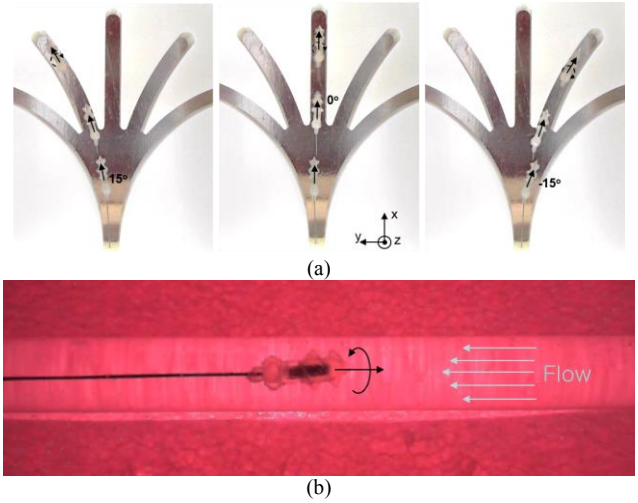

(a)

(b)

Figure 6. In-vitro experiment of the guide-wired microrobot; (a) locomotion and drilling motion in five branches phantom (4 mm in diameter) and (b) actuation and drilling motion in flow tube.

Future works will include in-vivo experiments to evaluate the clinical efficacy of the suggested mechanical thrombectomy device in this study.

References

[1] V. M. Pereira *et al.*, "Prospective, Multicenter, Single-Arm Study of Mechanical Thrombectomy Using Solitaire Flow Restoration in Acute Ischemic Stroke," *Stroke*, vol. 44, pp. 2802–2807, 2013.

[2] A. M. Spiotta, M. I. Chaudry, F. K. Hui, R. D. Turner, R. T. Kellogg, and A. S. Turk, "Evolution of thrombectomy approaches and devices for acute stroke: A technical review," *J. Neurointerv. Surg.*, vol. 7, no. 1, pp. 2–7, 2015.

[3] Y. P. Gobin *et al.*, "MERCI 1: A phase 1 study of mechanical embolus removal in cerebral ischemia," *Stroke*, vol. 35, no. 12, pp. 2848–2853, 2004.

[4] S. Takahashi *et al.*, "New method to increase a backup support of a 6 french guiding coronary catheter," *Catheter. Cardiovasc. Interv.*, vol. 63, no. 4, pp. 452–456, 2004.

[5] B. C. Campbell *et al.*, "Endovascular stent thrombectomy: the new standard of care for large vessel ischaemic stroke," *LANCET Neurol.*, vol. 14, no. 8, pp. 846–854, 2015.

[6] A. S. Turk *et al.*, "Initial clinical experience with the ADAPT technique: A direct aspiration first pass technique for stroke thrombectomy," *J. Neurointerv. Surg.*, vol. 6, no. 3, pp. 231–237, 2014.

[7] F. Carpi, N. Kastelein, M. Talcott, and C. Pappone, "Magnetically controllable gastrointestinal steering of video capsules," *IEEE Trans. Biomed. Eng.*, vol. 58, no. 2, pp. 231–234, 2011.

[8] K. R. J. Chun *et al.*, "Catheter ablation - New developments in robotics," *Herz*, vol. 33, no. 8, pp. 586–589, 2008.

[9] C. Jilek *et al.*, "Forces on cardiac implantable electronic devices during remote magnetic navigation," *Clin. Res. Cardiol.*, vol. 102, no. 3, pp. 185–192, 2013.

[10] A. D. Losey *et al.*, "Magnetically assisted remote-controlled endovascular catheter for interventional MR imaging: in vitro navigation at 1.5 T versus X-ray fluoroscopy," *Radiology*, vol. 271, no. 3, pp. 862–9, 2014.

[11] S. Jeong *et al.*, "Feasibility study on magnetically steerable guidewire device for percutaneous coronary intervention," *Int. J. Control. Autom. Syst.*, vol. 15, no. 1, pp. 473–479, 2017.

[12] S. Jeong, H. Choi, K. Cha, J. Li, J. O. Park, and S. Park, "Enhanced locomotive and drilling microrobot using precessional and gradient magnetic field," *Sensors Actuators, A Phys.*, vol. 171, no. 2, pp. 429–435, 2011.

[13] S. M. Jeon, G. H. Jang, H. C. Choi, S. H. Park, and J. O. Park, "Magnetic navigation system for the precise helical and translational motions of a microrobot in human blood vessels," *J. Appl. Phys.*, vol. 111, no. 7, pp. 1–4, 2012.

[14] H. Choi *et al.*, "EMA system with gradient and uniform saddle coils for 3D locomotion of microrobot," *Sensors Actuators, A Phys.*, vol. 163, no. 1, pp. 410–417, 2010.

[15] H. Choi *et al.*, "Electromagnetic actuation system for locomotive intravascular therapeutic microrobot," *5th IEEE RAS EMBS Int. Conf. Biomed. Robot. Biomechatronics*, pp. 831–834, 2014.

[16] H. Choi, K. Cha, S. Jeong, J. O. Park, and S. Park, "3-D locomotive and drilling microrobot using the novel stationary EMA system," *IEEE/ASME Trans. Mechatronics*, vol. 18, no. 3, pp. 1221–1225, 2013.

[17] C. Yu *et al.*, "Novel electromagnetic actuation system for three-dimensional locomotion and drilling of intravascular microrobot," *Sensors Actuators A Phys.*, vol. 161, no. 1–2, pp. 297–304, Jun. 2010.

[18] J. Nam, W. Lee, B. Jang, and G. Jang, "Magnetic Navigation System Utilizing Resonant Effect to Enhance Magnetic Field Applied to Magnetic Robots," *IEEE Trans. Ind. Electron.*, vol. 64, no. 6, pp. 4701–4709, 2017.